Article

Design and Application of Basic Amino Acids Displaying Enhanced Hydrophobicity

Juliana K. Kretsinger, and Joel P. Schneider

J. Am. Chem. Soc., **2003**, 125 (26), 7907-7913• DOI: 10.1021/ja029892o • Publication Date (Web): 04 June 2003

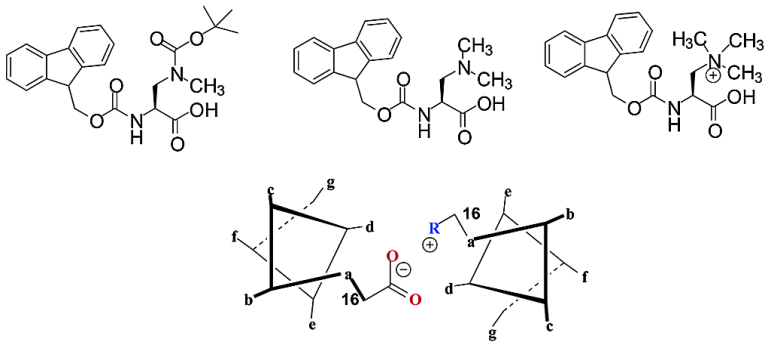

More About This Article

Additional resources and features associated with this article are available within the HTML version:

- Supporting Information
- Links to the 5 articles that cite this article, as of the time of this article download
- Access to high resolution figures
- Links to articles and content related to this article
- Copyright permission to reproduce figures and/or text from this article

View the Full Text HTML

J|A|C|S
ARTICLES
Published on Web 06/04/2003

Design and Application of Basic Amino Acids Displaying Enhanced Hydrophobicity

Juliana K. Kretsinger and Joel P. Schneider*

Contribution from the Department of Chemistry and Biochemistry, University of Delaware, Newark, Delaware 19716-2522

Received December 23, 2002; E-mail: schneijp@udel.edu

Abstract: Three noncoding basic amino acids, mono-, di-, and trimethyldiaminopropionic acid (mmdap, dmdap, and tmdap), have been synthesized for use in protein design. Covalent modification of a diaminopropionic acid (dap) side chain with an increasing number of methyl moieties results in a family of residues displaying short basic side chains with varying degrees of enhanced hydrophobic character. These residues may be used to introduce charged/polar interactions into the confining hydrophobic interior or interfacial spaces of proteins. As a demonstration of their utility, the ability of these residues to promote interior salt bridge formation at the helix/helix interface of GCN4-p1, a dimeric two-stranded coiled coil, was assessed. Heterodimerization mediated by buried salt bridge formation between a GCN4-based peptide containing either mmdap, dmdap, or tmdap at position 16 and an analogous peptide containing aspartic acid at the same position was studied. Mmdap-derived heterodimers are 0.5 kcal/mol more stable than the corresponding dap-derived heterodimers. This result indicates that the addition of one methyl group to the dap side chain can stabilize the heterodimeric fold. The stabilization can most likely be attributed to a decrease in the desolvation penalty incurred upon folding as well as enhanced van der Waals contacts in the folded state. The addition of three methyl groups to the dap side chain results in heterodimers that are significantly less stable than the corresponding dap-derived heterodimers, suggesting that increased steric bulk is not well accommodated in the interior of this protein. Unexpectedly, the addition of two methyl groups leads to homotrimerization of the dmdap-peptide. The resulting trimer is relatively stable ($\Delta G_{37°C}° = 11.8$ kcal/mol) and undergoes cooperative thermal unfolding. The GCN4-p1 system exemplifies how small incremental changes in size and hydrophobicity can alter the folding preferences of a protein. Generally, this versatile suite of residues can be utilized in any protein and offer new options to the protein chemist.

Introduction

Basic amino acid side chains contain hydrophobic regions which seem to contrast their polar/charged regions. Lysine, for example, contains four methylene groups capped by an ammonium ion at neutral pH. Although it is sometimes convenient to consider lysine as a hydrophilic residue, the apolar methylene groups of the residue often participate in favorable hydrophobic interactions within folded peptides and proteins.[1,2] In fact, the basic residues found in proteins are some of the largest residues, mostly due to their hydrophobic portions.

Nature has also found use for more compact basic residues with shortened side chains. For instance, the antituberculosis compound capreomycin (isolated from *Streptomyces capreolus*) and its active analogues contain two diaminopropionic acid (dap) residues, one of which is suggested to be important for biological activity.[3] Dap is also found in other antibiotics including edeine, viomycin, and the antitumor antibiotic, bleomycin.[4] Interestingly, when the two ^{D}phe residues of Gramicidin S are mutated to ^{D}dap, this antibiotic becomes active against gram-negative bacteria. Gramicidin S is typically active against gram-positive bacteria, and the change in selectivity is attributed to the incorporation of these residues into the hydrophilic face of this amphiphilic peptide.[5] Shortened basic residues have also found use in biophysical studies. For example, dap has been used to interrogate the snorkeling behavior of positively charged residues in transmembrane helices,[6] and both dap and diaminobutyric acid (dab) have been incorporated into solvent exposed regions of peptides to study helix propensity.[2]

In protein design, dap and dab residues can be used to introduce specific polar interactions into the protein matrix. For example, a buried salt bridge, formed from the association of a basic and acidic residue, may be incorporated into the hydrophobic interior of designed proteins to help specify a desired fold.[7] For this application, the compact dap and dab residues would seem to be ideal because they are small in size and meet the charge requirements of participating in the buried polar interaction. However, these compact residues, lacking the large

(1) Stites, W. E.; Gittis, A. G.; Lattman, E. E.; Shortle, D. *J. Mol. Biol.***1991**, *221*, 7−14.
(2) Groebke, K.; Renold, P.; Tsang, K. Y.; Allen, T. J.; McClure, K. F.; Kemp, D. S. *Proc. Natl. Acad. Sci. U.S.A.* **1996**, *93*, 4025−4029.
(3) Nomoto, S.; Shiba, T. *Bull. Chem. Soc. Jpn.* **1979**, *52*, 1709−15.
(4) Andruszkiewicz, R. *Pol. J. Chem.* **1995**, *69*, 1615−29.
(5) Ando, S.; Aoyagi, H.; Shinagawa, S.; Nishino, N.; Waki, M.; Kato, T.; Izumiya, N. *FEBS Lett.* **1983**, *161*, 89−92.
(6) Liu, F.; Lewis, R. N. A. H.; Hodges, R. S.; McElhaney, R. N. *Biochemistry* **2002**, *41*, 9197−9207.
(7) Schneider, J. P.; Lear, J. D.; DeGrado, W. F. *J. Am. Chem. Soc.* **1997**, *119*, 5742−5743.

10.1021/ja029892o CCC: $25.00

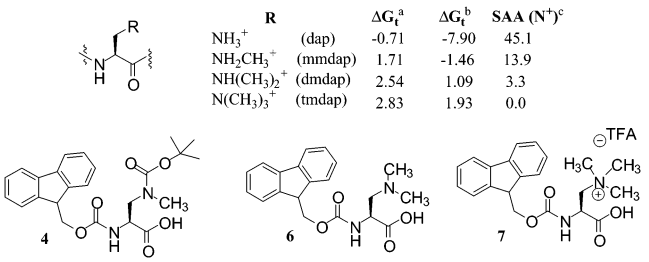

Figure 1. Structures of mono-, di-, and trimethylated analogues of diaminopropionic acid and the calculated transfer free energies (kcal/mol) for the protonated side chains of each residue for octanol/water[a] and vacuum/water[b] systems. [c]Calculated solvent-accessible area for the protonated N^{γ} atom (Å^2). Protected analogues **4**, **6**, and **7** were synthesized for use in Fmoc-based solid-phase peptide synthesis.

number of side-chain methylene moieties of their larger cousins, are relatively polar. As a result, their incorporation into the hydrophobic interior of a protein is expected to be energetically unfavorable.

In this paper, we report the synthesis and application of a family of noncoding basic residues that have shortened side chains and display enhanced hydrophobic character, Figure 1. These residues are analogues of dap in which an increasing number of methyl moieties are covalently incorporated at the side-chain nitrogen. Figure 1 shows calculated free energies for the transfer of each side chain from both octanol[8] and vacuum[9,10] into water. As the number the of N^{γ}-methyl groups increases, the ΔG_t's also increase, indicating an increase in hydrophobic character. Because the magnitude of ΔG_t is related to the solvent-accessible area (SAA) of each atom comprising a given side chain, the ability to decrease the SAA of the most hydrophilic atoms in the chain should effect the greatest change in ΔG_t. Calculated values of SAA for the positively charged side-chain nitrogen of each residue show that each methyl substituent is effective in incrementally decreasing the SAA of the protonated nitrogen atom and that two methyl groups are sufficient to effectively shield this atom from solvent, Figure 1. In regards to protein design, these residues fill a void in the existing palette of coding and noncoding residues as they are designed to fit well into protein interiors where a combination of charge and hydrophobicity is desired. Dap analogues **4**, **6**, and **7** were synthesized in a suitably protected form for facile incorporation into synthetic peptides via Fmoc-based solid-phase peptide synthesis (SPPS).

The utility of these residues is demonstrated herein by their incorporation into the hydrophobic interior of a small protein, GCN4-p1, to study their ability to support buried salt bridge formation. Buried salt bridges have been found to be conserved among members of several protein families, and the degree of conservation increases with decreasing solvent accessibility.[11] The ability of buried polar residues to hydrogen bond and participate in electrostatic interactions is often important in defining structural attributes.[12] In de novo protein design, the incorporation of a buried salt bridge can be used to drive the formation of a desired fold over alternate topologies. However,

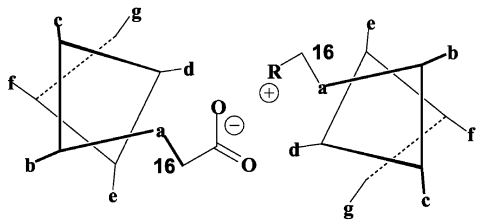

Peptide	Sequence
Mmdap-p1	Ac-RMKQLEDSKVEELLSK-**Mmdap**-YHLENEVARLKKLVGER-CONH$_2$
Dmdap-p1	Ac-RMKQLEDSKVEELLSK-**Dmdap**-YHLENEVARLKKLVGER-CONH$_2$
Tmdap-p1	Ac-RMKQLEDSKVEELLSK-**Tmdap**-YHLENEVARLKKLVGER-CONH$_2$
Dap-p1	Ac-RMKQLEDSKVEELLSK-**Dap**-YHLENEVARLKKLVGER-CONH$_2$
Asp-p1	Ac-RMKQLEDSKVEELLSK-**Asp**-YHLENEVARLKKLVGER-CONH$_2$

Figure 2. Helical wheel diagram of a parallel heterodimeric coiled coil showing the positions of a−g residues comprising one heptad repeat. Intended heterodimer formation is mediated via the buried salt bridge and may occur between the Asp-p1 peptide and any one of four peptides containing dap or the designed short basic residues.

incorporating a buried salt bridge usually leads to thermodynamic destabilization due to unfavorable desolvation contributions to the free energy incurred upon protein folding. The charged side chains forming a buried salt bridge must be desolvated for folding to occur.[13,14] Although buried salt bridges are associated with much higher desolvation costs than are solvent exposed bridges, buried bridges can compensate via stronger electrostatic interactions due to reduced solvent screening.[15] In addition to this compensatory effect, the unnatural residues presented here are designed to minimize the desolvation penalty due to their increased hydrophobic character.

GCN4-p1 is the 33 residue peptide spanning the leucine zipper portion of the yeast transcriptional activator protein, GCN4, and is known to fold as a parallel homodimeric coiled coil.[16] A single polar asparagine (asn) residue at position 16 of each helix comprising the homodimer specifies this fold by forming an interhelical hydrogen bond. Mutation of this partially buried asn16 to valine,[17] aminobutyric acid,[18] or glutamine[19] results in the formation of coiled coils of varying aggregation number, demonstrating the importance of this buried asparagine H-bond in specifying a single fold. In addition, it has been shown that a heterodimer can be specified by incorporating an interhelical salt bridge, where one helix contains an aspartic acid residue at position 16 and the other helix contains a dap residue at the same position, Figure 2. Although this buried salt bridge specifies a single fold, the resulting heterodimer is about 2 kcal/mol less stable than the wild-type homodimer.[7] The charged asp and dap residues forming the buried salt bridge of the heterodimer must become largely dehydrated upon folding. In comparison, wild-type GCN4-p1 only needs to dehydrate neutral asn residues to fold − an energetically less costly process.[20] Increasing the hydrophobicity of the basic residue involved in salt bridge formation should decrease this desol-

(8) Eisenberg, D.; McLachlan, A. D. *Nature* **1986**, *319*, 199−203.
(9) Sharp, K. A.; Nicholls, A.; Friedman, R.; Honig, B. *Biochemistry* **1991**, *30*, 9686−9697.
(10) Wesson, L.; Eisenberg, D. *Protein Sci.* **1992**, *1*, 227−235.
(11) Schueler, O.; Margalit, H. *J. Mol. Biol.* **1995**, *248*, 125−135.
(12) McClain, D. L.; Binfet, J. P.; Oakley, M. G. *J. Mol. Biol.* **2001**, *313*, 371−383.
(13) Hendsh, Z. S.; Tidor, B. *Protein Sci.* **1994**, *3*, 211−226.
(14) Hill, R. B.; Raleigh, D. P.; Lombardi, A.; DeGrado, W. F. *Acc. Chem. Res.* **2000**, *33*, 745−754.
(15) Kumar, S.; Nussinov, R. *J. Mol. Biol.* **1999**, *293*, 1241−1255.
(16) Oshea, E. K.; Klemm, J. D.; Kim, P. S.; Alber, T. *Science* **1991**, *254*, 539−544.
(17) Harbury, P. B.; Zhang, T.; Kim, P. S.; Alber, T. *Science* **1993**, *262*, 1401−1407.
(18) Gonzalez, L.; Brown, R. A.; Richardson, D.; Alber, T. *Nat. Struct. Biol.* **1996**, *3*, 1002−1010.
(19) Lino, G.; Woolfson, D. N.; Alber, T. *Nat. Struct. Biol.* **1996**, *3*, 1011−1018.
(20) Hendsch, Z. S.; Tidor, B. *Protein Sci.* **1999**, *8*, 1381−1392.

Scheme 1

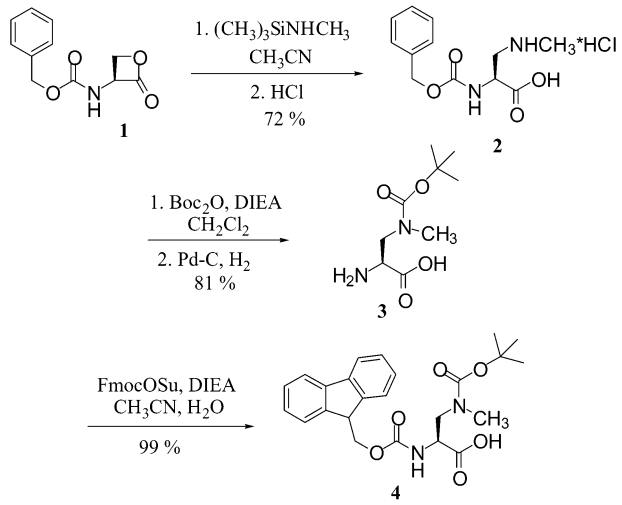

Scheme 2

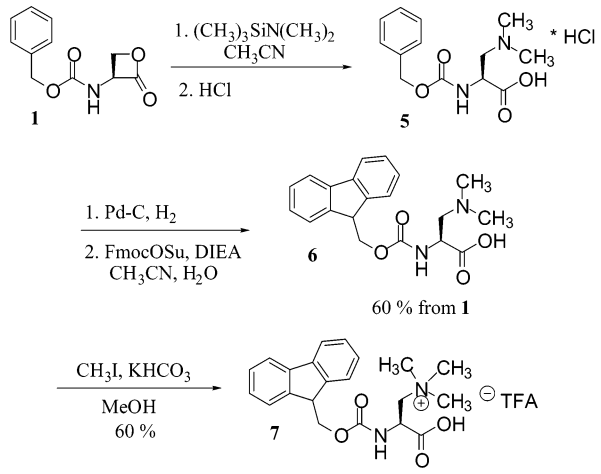

vation penalty. Here, we incorporate each of the dap analogues shown in Figure 1 into GCN4-p1 at position 16 and study their ability to form buried salt bridges upon heterodimer formation with the asp16 containing peptide, asp-p1 (Figure 2).

Results and Discussion

Synthesis. Fmoc-protected mono-, di-, and trimethyldiaminopropionic acid residues (Figure 1) were all prepared from β-lactone **1** as outlined in Schemes 1 and 2. Synthesis of the monomethyl analogue **4** is shown in Scheme 1. Ring opening of lactone **1** at the β-carbon with *N*-methyltrimethylsilylamine[21] in acetonitrile followed by acidic workup yielded the *Z*-protected monomethyl compound **2** in 72% yield. Treatment of **2** with di-*tert*-butyl dicarbonate followed by hydrogenation afforded amine **3** in 81% yield. Near quantitative incorporation of the Fmoc group yielded N^{α}-Fmoc-N^{β}-Boc-protected unnatural residue **4**. The synthesis of residue **6**, outlined in Scheme 2, began with the ring opening of lactone **1** with *N*,*N*-dimethyltrimethylsilylamine followed by acidic workup, yielding the *Z*-protected hydrochloride **5**. Fully characterized **5** was normally hydrogenated directly and Fmoc-protected, affording dimethyl analogue **6** in 60% yield from **1**. Last, the trimethyl analogue **7** was easily obtained via alkylation of **6** with methyl iodide.

GCN4-p1 peptide analogues containing substitutions at position 16 were prepared via automated SPPS, Figure 2. Residues **4** and **6** behaved ideally during automated SPPS and were incorporated using standard HBTU/HOBt activation chemistry affording peptides Mmdap-p1 and Dmdap-p1, respectively. However, the incorporation of residue **7** via SPPS proved problematic, and an alternate strategy was employed for the preparation of the corresponding peptide, Tmdap-p1. This peptide was most easily prepared by treating resin-bound Dmdap-p1 with methyl iodide under basic conditions. Because all of the side chains of Dmdap-p1 were protected, selective methylation of the dmdap residue was realized. Subsequent TFA-mediated cleavage from the resin and side-chain deprotection afforded Tmdap-p1. Care was taken in handling this peptide. Under neutral aqueous solution conditions, the unnatural side chain of Tmdap-p1 was prone to Hofmann elimination, affording dehydroalanine (half-life = 17 h at pH 7.0, 20 °C).[22] Under mildly acidic conditions (pH 6), elimination occurred at room temperature with a half-life greater than 3.5 days, and folding studies could be performed as long as they were accomplished in a timely manner. Although methylated variants of amino acids having longer side chains such as ornithine or lysine have been used in protein studies[33,34] and trimethylated derivatives would not be prone to β-elimination, their larger size precludes incorporation into most sterically demanding protein interiors.

The ability to perform elimination of the tmdap side chain quickly and cleanly with either base (pH > 8) or elevated temperatures may be of further interest. Dehydroalanine residues are found naturally in the active sites of some enzymes,[23,24] as well as in antibiotics of bacterial origin, including nisin[25] and subtilin.[26] These residues are additionally useful as electrophiles in the formation of nonnatural amino acids,[27] cyclic peptides,[28] and prenylated peptides.[29] In principle, tmdap is a synthon for dehydroalanine and can be used to introduce dehydroalanine into peptide sequences with exact temporal resolution (e.g., initiate elimination by raising the pH or temperature). Further study is underway to establish the potential advantages of this methodology.

Folding Attributes of Peptides. Homooligomerization. CD spectroscopy was used to probe the folding behavior of individual peptides to establish optimal solution conditions for studying heterodimerization. Figure 3a shows that Asp-p1, Mmdap-p1, and Dmdap-p1 adopted helical structure in a pH-dependent manner and that helical content was maximal at pH

(21) Ratemi, E. S.; Vederas, J. C. *Tetrahedron Lett.* **1994**, *35*, 7605−7608.
(22) Nomoto, S.; Sano, A.; Shiba, T. *Tetrahedron Lett.* **1979**, *20*, 521−522.
(23) Schwede, T. F.; Retey, J.; Schulz, G. E. *Biochemistry* **1999**, *38*, 5355−5359.
(24) Langer, B.; Roether, D.; Retey, J. *Biochemistry* **1997**, *36*, 10867−10871.
(25) Fukase, K.; Kitazawa, M.; Sano, A.; Shimbo, K.; Fujita, H.; Horimoto, S.; Wakamiya, T.; Shiba, T. *Tetrahedron Lett.* **1988**, *29*, 795−8.
(26) Gross, E.; Kiltz, H. H.; Craig, L. C. *Hoppe-Seyler's Z. Physiol. Chem.* **1973**, *354*, 799−801.
(27) Burkett, B. A.; Chai, C. L. L. *Tetrahedron Lett.* **1999**, *40*, 7035−7038.
(28) Okeley, N. M.; Zhu, Y.; van der Donk, W. A. *Org. Lett.* **2000**, *2*, 3603−3606.
(29) Zhu, Y.; van der Donk, W. A. *Org. Lett.* **2001**, *3*, 1189−1192.
(30) Boice, J. A.; Dieckmann, G. R.; DeGrado, W. F.; Fairman, R. *Biochemistry* **1996**, *35*, 14480−14485.
(31) Pansare, S. V.; Huyer, G.; Arnold, L. D.; Vederas, J. C. *Org. Synth.* **1992**, *70*, 1−9.
(32) Kim, J.; Bott, S. G.; Hoffman, D. M. *Inorg. Chem.* **1998**, *37*, 3835−3841.
(33) Demmers, J. A. A.; Rijkers, D. T. S.; Haverkamp, J.; Killian, J. A.; Heck, A. J. R. *J. Am. Chem. Soc.* **2002**, *124*, 11191−11198.
(34) Ashfield, J. T.; Meyers, T.; Lowne, D.; Varley, P. G.; Arnold, J. R. P.; Tan, P.; Yang, J. C.; Czaplewski, L. G.; Dudgeon, T.; Fisher, J. *Protein Sci.* **2000**, *9*, 2047−2053.

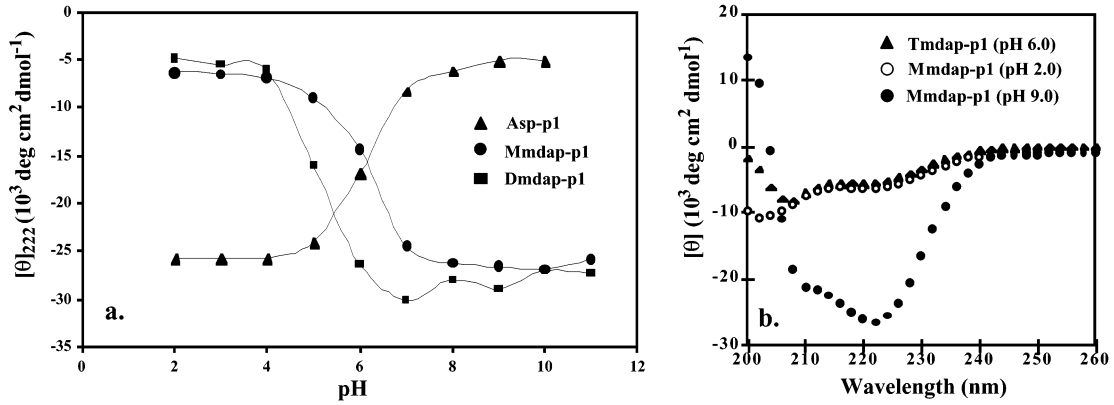

Figure 3. (a) pH-dependent folding as monitored by changes in θ_{222} for Mmdap-p1, Dmdap-p1, and Asp-p1. Peptide samples are 50 μM in 50 mM buffer, 150 mM NaCl. Buffers are glycine at pH 2 and 3, acetate at pH 4 and 5, MES at pH 6, BTP at pH 7, 8, and 9, and CAPS at pH 10 and 11. (b) CD spectra of 100 μM solution of Tmdap-p1 at pH 6.0 and 50 μM solutions of Mmdap-p1 at pH 2.0 and 9.0. Buffers as defined in (a).

values in which the side chains of the residues at position 16 were in their nonionized, neutral states. This pH-dependent behavior is expected as electrostatic repulsion will disfavor homooligomerization when the side chains at position 16 are ionized. Under folding conditions, sedimentation equilibrium analytical ultracentrifugation (SEAU) experiments indicated that Asp-p1 and Mmdap-p1 formed homodimers and Dmdap-p1 formed a homotrimer (see Supporting Information). Tmdap-p1 is not included in panel a because β-elimination of the tmdap side chain occurs under basic solution conditions (vide supra). Knowing that tmdap contains a quaternary amine, it must be positively charged at all pH's, and consequently Tmdap-p1 should be monomeric and unstructured. In fact, the CD spectrum of Tmdap-p1 at pH 6.0 was indicative of random coil, closely resembling unfolded Mmdap-p1, Figure 3b.

Heterooligomerization. Solution conditions that promote heterodimerization between Asp-p1 and the base-containing peptides are those in which the side chains at position 16 are fully ionized and homooligomerization is disfavored. The data in Figure 3a suggest that a compromise must be met in choosing the optimal pH to drive heterodimer formation as no pH value exists where both the asp and the amine-containing side chain will be fully ionized. Heterodimerization of Mmdap-p1 with Asp-p1 was studied at pH 6.0, where the maximal amounts of each peptide bear charged side chains at position 16. For consistency, heterodimerization of Tmdap-p1 with Asp-p1 was also studied at pH 6.

Assessing the ability of the dmdap residue to support buried salt bridge formation in the context of GCN4-based heterodimerization was not possible. It is apparent from Figure 3a that the intrinsic pK_a of the dmdap side chain was significantly depressed in comparison to the mmdap side chain. Therefore, no pH value exists in which homooligomerization was not favored for either the Asp-p1 or the Dmdap-p1 peptides, and all attempts to coax heterodimerization failed. An explanation for the inability of Dmdap-p1 to form heterodimers can be derived from thermal denaturation experiments (described below), which indicated that homotrimerization of Dmdap-p1 was a much more favorable process than salt bridge-mediated heterodimerization. However, this observation does not mean that the dmdap residue is limited in its ability to form energetically favorable buried salt bridges. It only means that GCN4-p1 may not be the optimal model system to study dmdap-based salt bridge formation; this residue may be ideal for

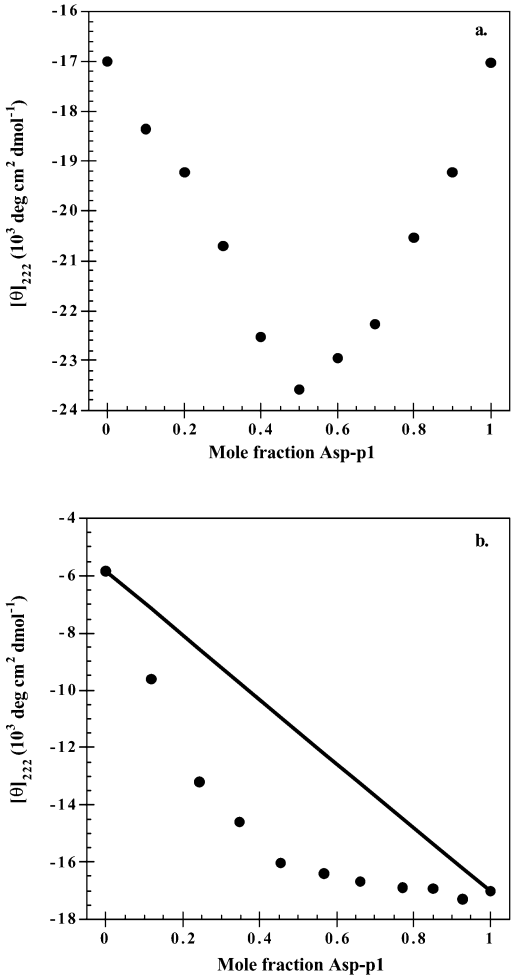

Figure 4. Mole fraction titration of (a) Mmdap-p1 and (b) Tmdap-p1 with Asp-p1. Total peptide concentration is 50 μM in 50 mM MES, 150 mM NaCl, pH 6.0. In panel b, a line is included to show the expected $[\theta]_{222}$ values if no interaction occurred between the two peptides.

incorporation into monomeric proteins or proteins whose olimerization state is not as sensitive to structural changes as GCN4-p1.[17]

Heterodimer formation of Asp-p1 with Mmdap-p1 and Tmdap-p1 was initially indicated by mole fraction titration experiments performed at pH 6.0 (Figure 4). In Figure 4a, a distinct minimum is seen at a 1:1 molar ratio of Mmdap-p1 to

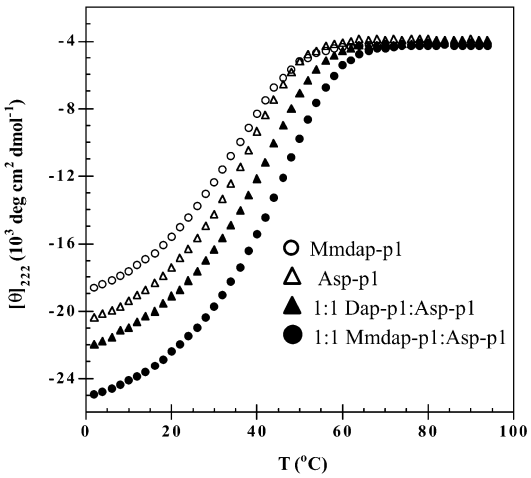

Figure 5. Thermal denaturations monitored by CD for homo- and heterogeneous solutions of peptides. Total peptide concentration is 100 μM in 50 mM Mes, 150 mM NaCl, pH 6.0.

Asp-p1, suggesting heterodimerization. Figure 4b suggests heterodimer formation for the Tmdap-p1:Asp-p1 pair as well, although the heterodimer exhibited approximately the same mean residue ellipticity as the Asp-p1 homodimer. Importantly, SEAU of 1:1 mixtures of Mmdap-p1:Asp-p1 and Tmdap-p1:Asp-p1 showed the expected apparent molecular weights for heterodimer formation (see Supporting Information).

Thermodynamic Assessment. By design, increasing the side-chain hydrophobicity of the amine containing peptide should result in the formation of heterodimers exhibiting increased stability. Figure 5 compares thermal unfolding curves for equimolar mixtures of the Dap-p1:Asp-p1 and the Mmdap-p1:Asp-p1 pairs. As compared to Dap-p1:Asp-p1, the unfolding curve for the Mmdap-p1:Asp-p1 solution shifted to higher temperatures and exhibited greater helicity at low temperatures. Qualitatively, this suggests that the Mmdap-p1:Asp-p1 heterodimer enjoyed enhanced thermal stability as a result of incorporating the additional methyl moiety. Figure 5 also demonstrates that at pH 6 homogeneous solutions of Mmdap-p1 and Asp-p1 formed marginally stable homodimers. The data in Figure 5 as well as concentration-dependent data (see Supporting Information) were globally fit to the Gibbs−Helmholtz equation. Equilibrium constants were first determined for each competing homodimer. Once these values were known, thermal denaturation data resulting from appropriate heterogeneous mixtures were fit to competing equilibria, and heterodimer equilibrium constants were determined. The results provided in Table 1 show that, for both the Dap-p1:Asp-p1 and the Mmdap-p1:Asp-p1 solutions, heterodimerization was preferred over competing homodimerization by 2.0 kcal/mol ($\Delta\Delta G_{\text{specificity}}°$). The degree of specificity was insensitive to electrolyte concentration, suggesting that the Mmdap-p1:Asp-p1 salt bridge was sufficiently shielded from solvent, Table 1. Importantly, at 37 °C and 150 mM NaCl, the Mmdap-p1:Asp-p1 heterodimer was 0.5 kcal/mol more stable than the corresponding Dap-p1:Asp-p1 dimer ($\Delta G°$ of 7.2 versus 6.7 kcal/mol). The incorporation of one methyl group into the amine side chain resulted in a more stable heterodimer presumably due to a decrease in the desolvation penalty experienced upon folding.

Conceptually, amine side chains bearing multiple methyl groups should further decrease the desolvation penalty, and their

Table 1. Thermodynamic Assessment of Oligomerization

peptide	NaCl (M)	$\Delta G°$ (37 °C)[a] (kcal/mol)	$\Delta\Delta G_{\text{spec}}°$ [b] (kcal/mol)	T_m (1 M)[c] (°C)	T_m (100 μM)[d] (°C)
Asp-p1	0.15	5.4		74.9	31.7
Dap-p1	0.15	3.8		66.6	−0.7
Mmdap-p1	0.15	5.1		75.6	28.5
Dap-p1:Asp-p1	0.15	6.7	2.1	86.6	44.2
Mmdap-p1:Asp-1	0.15	7.2	2.0	94.0	48.8
Mmdap-p1:Asp-1	0.025	7.1	1.9	93.5	49.0
Mmdap-p1:Asp-1	0.5	7.2	2.0	95.9	49.7
Dmdap-p1	0.15	11.5		99.4	73.0

[a] $\Delta G°$ was determined from thermal denaturation of indicated peptides (100 μM, pH 6.0, 50 mM MES) monitored by CD at 222 nm (standard state = 1 M); the uncertainties in $\Delta G°$ and T_m are ±0.1 kcal mol^{-1} and 1 °C, estimated by sensitivity analysis of the theoretical curves. [b] $\Delta\Delta G_{\text{spec}}° = \Delta G°ab - {}^1/_2[\Delta G°aa + \Delta G°bb]$. T_m extrapolated to the standard state (1 M)[c] and at 100 μM total peptide concentration,[d] where T_m is the temperature at which $\Delta G = 0$.

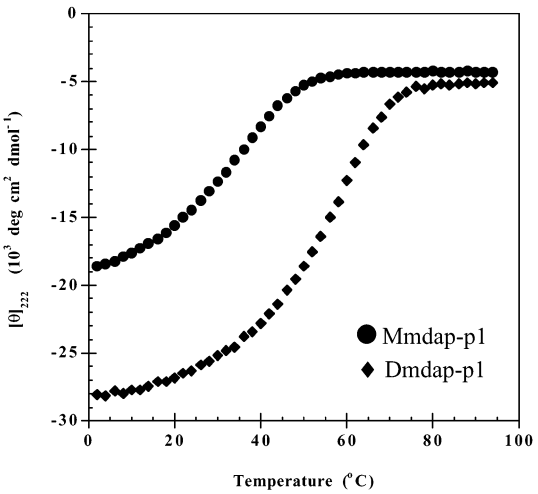

Figure 6. Themal denaturations monitored by CD for 100 μM homogeneous solutions of Mmdap-p1 and Dmdap-p1 in 50 mM MES, 150 mM NaCl, pH 6.0.

corresponding heterodimers should exhibit increased stability. However, this linear extrapolation in thought negates additional factors important for proper folding such as sterics. In fact, the incorporation of a dmdap residue, whose side chain bears two methyl moieties, into the GCN4-p1 scaffold afforded a peptide (Dmdap-p1) incapable of forming heterodimers with Asp-p1. Instead, Dmdap-p1 formed homotrimers as evident by SEAU. This aggregation state can better accommodate the steric bulk of the additional methyl group. Dmdap-p1-derived homotrimers underwent a cooperative, reversible two-state thermal unfolding/folding transition reminiscent of nativelike proteins, Figure 6. A fit of the unfolding curve invoking a trimer−monomer equilibrium afforded a $\Delta G°$(37 °C) of 11.8 kcal/mol (1 M standard state), indicating that the trimer was of moderate stability.[30] Although there are no reports of a GCN4-p1 single mutant containing the isostructural residue leucine at position 16, one would predict that such a mutant would favor the formation of trimers based on the observed aggregation state of Dmdap-p1.

The GCN4-p1 scaffold seems to be rather unyielding in accommodating steric challenges to its interior. Although Tmdap-p1 was capable of forming heterodimers with Asp-p1, the helicity of the resultant heterodimers is only 75% that of the Mmdap-p1-derived heterodimers, Figure 4. Chemical denaturation studies employing guanidine hydrochloride (see

Supporting Information) demonstrated that the Tmdap-p1:Asp-p1 heterodimer is relatively unstable, suggesting that the trimethylammonium side chain was not easily accommodated into the protein interior.

Conclusion

Three Fmoc-protected amino acids (**4**, **6**, and **7**) have been prepared, and their potential utility in protein design has been explored. These mono-, di-, and trimethylated diaminopropionic acid derivatives were designed such that each additional methyl moiety covalently incorporated at the side-chain nitrogen serves to incrementally increase the hydrophobicity of the residue. The result is a suite of residues whose side chains offer ammonium ions capable of engaging in polar/charged interactions, but contradictorily express enhanced hydrophobic character. These residues may be used to introduce polar functionality into the interior of designed proteins while simultaneously offering nonpolar surface area for easier accommodation into hydrophobic environments. The utility of these residues has been explored here via the construction of buried salt bridges into the coiled coil scaffold of GCN4-p1.

Experimental Section

General Methods and Materials. (*Z*)-Serine β-lactone **1** was synthesized from (*Z*)-serine according to the procedure of Pansare et al.[31] *N*-Methyltrimethylsilylamine was synthesized according to the procedure of Kim et al.[32] Ultrapure Gdn HCl was purchased from ICN. Palladium on carbon and *N*-(9*H*-fluoren-2-ylmethoxycarbonyloxy)-succinimide (Fmoc-OSu) were purchased from Acros Organics. Fmoc-protected amino acids, 2-(1*H*-benzotriazole-1-yl)-1,1,3,3-tetramethyl-uronium hexafluorophosphate (HBTU), *N*-hydroxybenzotriazole (HOBT), piperidine, *N*-methylpyrrolidone, and amide resin were purchased from Applied Biosystems. Methyl iodide was filtered through alumina prior to use. Solvents were purchased from Fisher Scientific and used without further purification except the acetonitrile and dichloromethane, which were distilled from calcium hydride. *N*,*N*-Dimethyltrimethylsilylamine and the remaining chemicals were purchased from Aldrich and used as received.

Synthesis of (*Z*)-Monomethyl Diaminopropionic Acid·HCl 2. Under nitrogen atmosphere, a dry round-bottomed flask was charged with *N*-methyltrimethylsilylamine (3.0 g, 29 mmol) followed by 10 mL of dry acetonitrile. A solution of (*Z*)-serine β-lactone **1** (5 g, 22.6 mmol) in 9 mL of dry acetonitrile was added via syringe. The resulting solution was stirred at room temperature for 12 h, subsequently cooled in an ice bath, and 100 mL of cold 0.1 M HCl was then added to reduce the pH to 2−3. The resulting solution was stirred and allowed to warm to room temperature over 30 min, transferred to a separatory funnel, and washed with CH_2Cl_2 (4 × 100 mL) and diethyl ether (2 × 100 mL) to remove undesired carbonyl ring-opened amide. The aqueous layer was then rotary evaporated, yielding 4.7 g of (*Z*)-monomethyl diaminopropionic acid·HCl **2** (16.3 mmol, 72%) as a light yellow foam. ^{1}H NMR (D_2O, 400 MHz): δ 7.43 (m, 5H), 5.12 (s, 2H), 4.30 (dd, J = 5.6 and 8.2, 1H), 3.42 (dd, J = 5.4 and 12.9, 1H), 3.24 (dd, J = 8.5 and 12.8, 1H), 2.73 (s, 3H). ^{13}C NMR (D_2O, 100 MHz): δ 171.73, 157.81, 138.05, 129.85, 129.38, 128.27, 68.08, 52.16, 50.67, 45.44, 34.75. HRMS (ESI) *m*/*z* 253.1186 [(M + H$^+$), calcd for $C_{12}H_{17}N_2O_4^+$ 253.1188].

Synthesis of Monomethylamine 3. Under a nitrogen atmosphere, a 200 mL round-bottomed flask was charged with *Z*-protected monomethylamine hydrochloride **2** (4.7 g, 16.3 mmol) and 82 mL of dry methylene chloride. The mixture was stirred, cooled via an ice bath, and diisopropyl ethylamine (DIEA) (17.0 mL, 97.8 mmol) was added slowly via pipet. The ice bath was removed, and $(Boc)_2O$ (3.73 g, 17.1 mmol) was added at once as a solid. After being stirred for 5 h at room temperature, the reaction solution was transferred to a separatory funnel, washed with 0.1 M citric acid (3 × 30 mL), water (1 × 30 mL), dried (Na_2SO_4), and concentrated under reduced pressure to yield an oil. The oil was bathed in hexanes to remove residual $(Boc)_2O$ and dried under vacuum for 1 h. The resulting oil was then dissolved in 150 mL of methanol, and 10% Pd/C (0.3 g) was added. This mixture was stirred under a balloon of H_2 for 1.5 h after which time the reaction mixture was filtered, concentrated, and the resulting oil triturated with acetonitrile to afford a white precipitate which was collected by filtration and dried under vacuum yielding 2.88 g of monomethylamine **3** (13.2 mmol, 81%). ^{1}H NMR (D_2O, 400 MHz): δ 3.90 (dd, J = 7.5 and 4.3 Hz, 1H), 3.79 (m, 1H), 3.65 (dd, J = 15 and 7.6 Hz, 1H), 2.87 (br d, 3H, cis/trans isomers), 1.44 (s, 9H). ^{13}C NMR (D_2O, 100 MHz): δ 172.57, 157.73, 83.12, 54.18, 49.97, 35.03, 27.95. HRMS (ESI) *m*/*z* 241.1161 [(M + Na)$^+$, calcd for $C_9H_{18}N_2O_4$ Na, 241.1164].

Synthesis of Fmoc-Protected Monomethylamine 4. A 100 mL round-bottomed flask was sequentially charged with monomethylamine **3** (1.0 g, 4.59 mmol), 12 mL of acetonitrile, 12 mL of water, Fmoc-OSu (1.56 g, 4.63 mmol), and 2.38 mL of DIEA (13.8 mmol). The reaction mixture was stirred at room temperature for 5 h, after which time the solvent was removed by evaporation. The resulting oil was partitioned between 30 mL of ethyl acetate and 30 mL of 0.1 M citric acid. The aqueous and organic phases were separated, and the organic phase was subsequently washed with 0.1 M citric acid (2 × 30 mL), water (1 × 30 mL), dried (Na_2SO_4), and concentrated under reduced pressure to yield 2.0 g of **4** as an oil after drying on high vacuum (4.54 mmol, 99%). ^{1}H NMR ($(CD_3)_2SO$, 400 MHz): δ 7.89 (d, J = 7.5, 2H), 7.71 (d, J = 7.2, 2H), 7.41 (t, J = 7.4, 2H), 7.32 (t, J = 7.4, 2H), 4.30−4.20 (m, 4H), 3.65 (m, 1H), 3.37 (bs, 1H), 3.29 (m, 1H), 2.78 (bd, 3H, cis/trans isomers). ^{13}C NMR ($(CD_3)_2SO$, 100 MHz): δ 172.24, 156.00, 154.53, 143.77, 140.76, 127.69, 127.11, 125.26, 120.18, 78.85, 65.70, 52.54, 49.41, 46.65, 34.96, 27.96. HRMS (ESI) *m*/*z* 463.1832 [(M + Na$^+$), calcd for $C_{24}H_{28}NO_4Na^+$ 463.1845].

Synthesis of (*Z*)-Dimethyl Diaminopropionic Acid 5. Under nitrogen atmosphere, a dry 100 mL round-bottomed flask was charged with (*Z*)-serine β-lactone **1** (1.0 g, 4.5 mmol) and 60 mL of dry acetonitrile, followed by *N*,*N*-dimethyltrimethylsilylamine (0.762 mL, 4.7 mmol) via syringe. The reaction was stirred at room temperature for 2 h, monitoring the disappearance of **1** (R_f = 0.68) by TLC (85:15; $CHCl_3$:MeOH). After completion, the reaction was cooled in an ice bath, and 100 mL of 0.1 N HCl was added. The resulting solution was stirred and allowed to warm to room temperature over 30 min, transferred to a separatory funnel, and washed with CH_2Cl_2 (3 × 100 mL). The aqueous layer was lyophilized to afford ∼1.2 g of **5** which normally contains a moderate amount of dimethylamine hydrochloride salt byproduct. Although the salt was generally taken directly to the next step, product free from salt can be obtained using a Waters Sep-Pak Vac 35 cm^3 (10 g) C18 cartridge. ^{1}H NMR (CD_3CN, 400 MHz): δ 7.3 (m, 5H), 6.89 (d, J = 6.6 Hz, 1H), 5.08 (s, 2H), 4.39 (m, 1H), 3.34 (d, J = 7.1 Hz, 2H), 2.77 (s, 6H). ^{13}C NMR (CD_3CN, 100 MHz): δ 173.24, 157.31, 138.09, 129.54, 129.00, 128.84, 67.35, 57.79, 51.21, 43.97. HRMS (ESI) *m*/*z* 267.1342 [(M + H$^+$), calcd for $C_{13}H_{19}N_2O_4^+$ 267.1345].

Synthesis of Fmoc-Dimethyl Diaminopropionic Acid 6. A 250 mL round-bottomed flask containing 1.2 g of crude (*Z*)-dimethyl diaminopropionic acid **5** was charged with 225 mL of MeOH and 0.14 g of 10% Pd/C. Hydrogen was bubbled through the solution while it was stirred for 1 h. The Pd/C was removed by gravity filtration, and rotary evaporation of the filtrate afforded an oily solid. This oil was dissolved in 40 mL of 50% acetonitrile/water, and DIEA was added until a constant pH of 9 was obtained. Next, Fmoc-OSu (1.5 g, 4.4 mmol) was added at once, and the reaction was stirred at room temperature for 5 h. The resulting solution was washed with diethyl ether (3 × 40 mL), and the aqueous layer was lyophilized to afford crude **6** which was purified using a Waters Sep-Pak Vac 35 cm^3 (10 g) C18 cartridge. Crude **6** was loaded onto the Sep-Pak in water as a

suspension and washed with 15 mL of water. The product was then eluted with 50% acetonitrile/water and lyophilized to afford 0.96 g (2.7 mmol, 60%) of **6** as a white solid. ^{1}H NMR (CD_3CN, 400 MHz): δ 7.82 (d, $J = 7.6$ Hz, 2H), 7.66 (m, 2H), 7.41 (t, $J = 7.4$ Hz, 2H), 7.33 (m, 2H), 6.19 (m, 1H), 4.35 (d, $J = 6.7$, 2H), 4.23 (t, $J = 6.7$, 1H), 4.08 (m, 1H), 3.17 (dd, $J = 5.1$ and 12.04, 1H), 2.98 (m, 1H), 2.72 (s, 5H), 2.35 (bs, 1H). ^{13}C NMR (CD_3CN, 100 MHz): δ 173.30, 157.54, 145.43, 142.43, 129.06, 128.49, 126.58, 121.33, 67.79, 59.13, 51.05, 48.27, 44.28. HRMS (ESI) *m*/*z* 355.1662 [($M + H^+$), calcd for $C_{20}H_{23}N_2O_4^+$ 355.1658].

Synthesis of Fmoc-Trimethyl Diaminopropionic Acid 7. A dry round-bottomed flask was sequentially charged with **6** (0.79 g, 2.2 mmol), 22 mL of methanol, $KHCO_3$ (267 mg, 2.7 mmol), and methyl iodide (1.58 g, 11.1 mmol). The reaction mixture was stirred under an atmosphere of nitrogen at room temperature for 26 h and subsequently transferred to a separatory funnel where 20 mL of water was added. The aqueous solution was washed with CH_2Cl_2 (1 × 20 mL), and the aqueous fraction was lyophilized to afford 1.23 g of crude **7**. The product was purified by reverse phase HPLC (C18 Vydac peptide/protein column) employing a linear gradient of solvent B (where solvent A was composed of water and 0.1% TFA, and solvent B was composed of 90% acetonitrile, 10% water, and 0.1% TFA) to afford 0.64 g (1.3 mmol) of **7** as a white solid. ^{1}H NMR (CD_3CN, 400 MHz): δ 7.80 (d, $J = 7.5$ Hz, 2H), 7.67 (d, $J = 7.5$ Hz, 2H), 7.40 (t, $J = 7.4$ Hz, 2H), 7.32 (dt, $J = 7.4$, 2H), 4.73 (d, $J = 7.2$, 2H), 4.61 (dd, $J = 6.2$ and 10.76, 1H), 4.53 (dd, $J = 6.0$ and 10.75, 1H), 4.25 (t, $J = 6.1$, 1H), 4.01 (dd, $J = 2.3$ and 13.9, 1H), 3.58 (dd, $J = 8.8$ and 13.9, 1H), 3.31 and 3.13 (two singlets are observed due to side-chain conformational isomerization; total integration 9H). ^{13}C NMR (CD_3CN, 100 MHz): δ 170.48, 158.82, 143.76, 140.83, 127.73, 127.13, 125.17, 120.22, 65.70, 65.60, 52.86, 49.47, 46.73. HRMS (ESI) *m*/*z* 369.1827 [(M^+), calcd for $C_{21}H_{25}N_2O_4^+$ 369.1814].

Peptide Synthesis. Peptides were synthesized on amide resin using an ABI 433A peptide synthesizer employing HBTU/HOBT activation. Peptide N-termini were acetylated using acetic anhydride and DIEA. Resin-bound peptides were cleaved and deprotected via treatment with 90% TFA, 5% thioanisole, 3% ethanedithiol, 2% anisole for 4 h under nitrogen atmosphere. Peptides were purified by RP-HPLC (Vydac C4 or C18 peptide/protein column) employing linear gradients of solvent B. Mass spectroscopy data can be found in the Supporting Information. The molecular weights reported here are calculated using the multiple charge states observed from electrospray ionization. Mmdap-p1, ESI (M) calcd 4023.7, obsd 4023.6; Dmdap-p1, ESI (M) calcd 4037.8, obsd 4038.0; Dap-p1, ESI (M) calcd 4009.7, obsd 4009.5; Asp-p1, ESI (M) calcd 4038.7, obsd 4038.0.

Synthesis of Tmdap-p1. A dry 5 mL pear-shaped flask equipped with a stirbar was charged with resin-bound Dmdap-p1 (130 mg; Ld = 0.127 mmol/g) and 1.5 mL of anhydrous DMF. 1,3,4,6,7,8-Hexahydo-1-methyl-2*H*-pyrimido[1,2-*a*]-pyrimidine (MTBD) (2.86 μL, 19.9 μmol) was added to the swollen resin-bound peptide followed by methyl iodide (23.6 mg, 166 μmol). The resin slurry was stirred for 4 h under an atmosphere of nitrogen, after which time the resin-bound peptide was filtered and washed with DMF (3 × 10 mL), DCM (3 × 10 mL), and dried under vacuum. Treatment of resin bound peptide with 90% TFA, 5% thioanisole, 3% ethanedithiol, 2% anisole for 2 h under nitrogen atmosphere affords pure Tmdap-p1 after RP-HPLC purification (yields determined by HPLC ranged from 50% to 90% depending on starting material purity). ESI $(M)^+$ calcd 4051.8, obsd 4052.0.

CD Spectroscopy. All experiments were performed on an Aviv model 62DS circular dichroism spectropolarimeter. Sample concentrations were determined by UV absorbance of the tyrosine residue (ϵ_{275} = 1450 cm^{-1} M^{-1}). Wavelength scans were recorded using a 2 nm step size and a 15 s average time. Thermal denaturation experiments were monitored at 222 nm from 2 to 94 °C in 2 °C steps with a 4 min equilibration time and data averaging for 60 s at each temperature. Thermodynamic parameters were determined via global fits of thermal denaturation curves as previously described.[7] A Microlab 500 series automated titrator was used for the guanidine hydrochloride denaturation experiments; peptide concentration was held constant, while the Gdn HCl concentration was increased from 0 to 3.5 M in 0.1 M increments, and then from 3.5 to 7 M in 0.25 M increments. Data were collected and averaged for 10 s after 1 min stirring and 20 s settling.

Sedimentation Equilibrium Analytical Ultracentrifugation. SEAU data were collected at 20 °C on a Beckman XL-I Analytical ultracentrifuge with an An-60 Ti rotor. Sample concentrations were determined by tyrosine absorbance (ϵ_{275} = 1450 cm^{-1} M^{-1}). Cell length-dependent absorbance measurements at 275 nm were made at three rotor speeds (32 000, 37 000, and 42 000 rpm). The resulting data were fit globally as previously described[7] using the software package Igor Pro (WaveMetrics, Inc.).

Acknowledgment. We would like to thank Dan Camac and Jim Lear for helpful discussions. This work was supported in part by ACS PRF-G: 36376-G4 (J.P.S.).

Supporting Information Available: Index, mass spectroscopy, denaturation, and SEAU data for all peptides (PDF). This material is available free of charge via the Internet at http://pubs.acs.org.

JA029892O